Sea spray geoengineering experiments in the geoengineering model intercomparison project (GeoMIP): Experimental design and preliminary results

Ben Kravitz,[1] Piers M. Forster,[2] Andy Jones,[3] Alan Robock,[4] Kari Alterskjær,[5] Olivier Boucher,[6] Annabel K. L. Jenkins,[2] Hannele Korhonen,[7] Jón Egill Kristjánsson,[5] Helene Muri,[5] Ulrike Niemeier,[8] Antti-Ilari Partanen,[7] Philip J. Rasch,[1] Hailong Wang,[1] and Shingo Watanabe[9]

[1] Marine cloud brightening through sea spray injection has been proposed as a method of temporarily alleviating some of the impacts of anthropogenic climate change, as part of a set of technologies called geoengineering. We outline here a proposal for three coordinated climate modeling experiments to test aspects of sea spray geoengineering, to be conducted under the auspices of the Geoengineering Model Intercomparison Project (GeoMIP). The first, highly idealized, experiment (*G1ocean-albedo*) involves a uniform increase in ocean albedo to offset an instantaneous quadrupling of CO_2 concentrations from preindustrial levels. Results from a single climate model show an increased land-sea temperature contrast, Arctic warming, and large shifts in annual mean precipitation patterns. The second experiment (*G4cdnc*) involves increasing cloud droplet number concentration in all low-level marine clouds to offset some of the radiative forcing of an RCP4.5 scenario. This experiment will test the robustness of models in simulating geographically heterogeneous radiative flux changes and their effects on climate. The third experiment (*G4sea-salt*) involves injection of sea spray aerosols into the marine boundary layer between 30°S and 30°N to offset $2\,\mathrm{W\,m^{-2}}$ of the effective radiative forcing of an RCP4.5 scenario. A single model study shows that the induced effective radiative forcing is largely confined to the latitudes in which injection occurs. In this single model simulation, the forcing due to aerosol-radiation interactions is stronger than the forcing due to aerosol-cloud interactions.

1. Introduction

[2] Solar geoengineering, also called Solar Radiation Management, has been proposed as a method of temporarily alleviating some of the climate effects of anthropogenic CO_2 emissions by reducing the amount of net solar irradiance reaching Earth [e.g., *Crutzen*, 2006]. One such method of solar geoengineering is via brightening of marine stratocumulus clouds [*Latham*, 1990, 2002].

[3] A large source of cloud condensation nuclei (CCN) in marine low clouds is from sea spray [*Lewis and Schwartz*, 2004]. The theoretical aerosol-cloud interactions resulting from the introduction of CCN into these clouds are often divided into two dominant effects. The first is that for constant cloud liquid water content, an increase in CCN also increases cloud droplet number concentration (CDNC), redistributing the available water among more droplets, forming smaller droplets [*Twomey*, 1974, 1977]. This increases cloud optical thickness, and hence, cloud albedo. The second effect relies on the hypothesis that introducing aerosol particles of a certain size range into marine low clouds can homogenize the cloud droplet size distribution. These smaller droplets have lower collision-coalescence efficiencies, reducing precipitation efficiency and thus increasing cloud amount and lifetime [*Albrecht*, 1989]. Both of these effects have been observed, most notably in the form of ship tracks [e.g., *Christensen and*

————————
[1]Atmospheric Sciences and Global Change Division, Pacific Northwest National Laboratory, Richland, Washington, USA.
[2]School of Earth and Environment, University of Leeds, Leeds, UK.
[3]Met Office Hadley Centre, Exeter, UK.
[4]Department of Environmental Sciences, Rutgers University, New Brunswick, New Jersey, USA.
[5]Department of Geosciences, University of Oslo, Oslo, Norway.
[6]Laboratoire de Météorologie Dynamique, IPSL, CNRS/UPMC, Paris, France.
[7]Kuopio Unit, Finnish Meteorological Institute, Kuopio, Finland.
[8]Max Planck Institute for Meteorology, Hamburg, Germany.
[9]Japan Agency for Marine-Earth Science and Technology, Yokohama, Japan.

Corresponding author: B. Kravitz, Atmospheric Sciences and Global Change Division, Pacific Northwest National Laboratory, P. O. Box 999, MSIN K9-24, Richland, WA 99352, USA. (ben.kravitz@pnnl.gov)
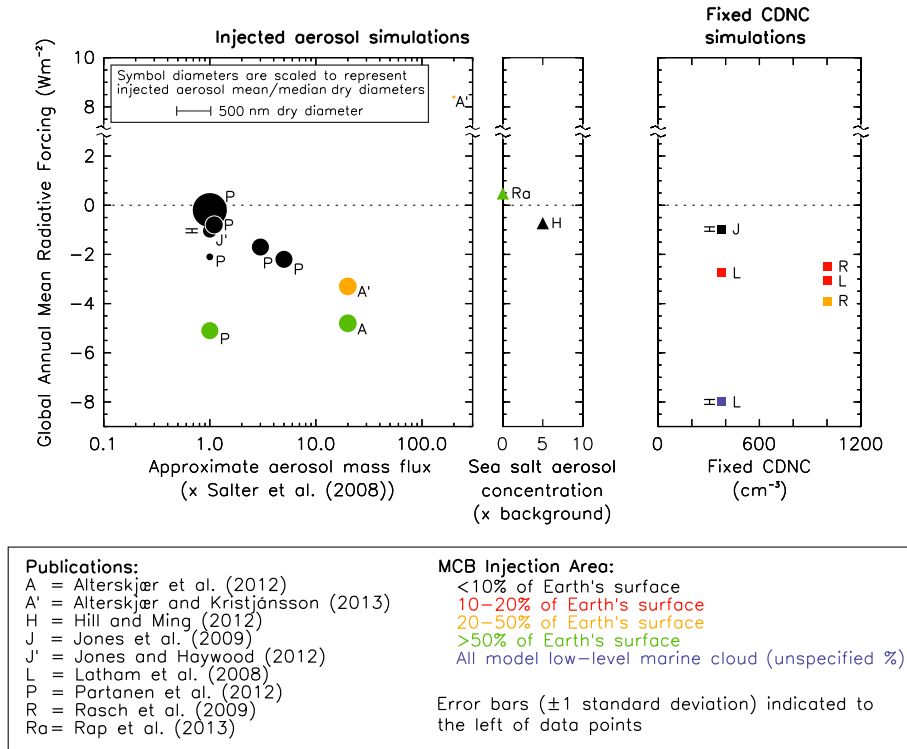
Figure 1. Summary of radiative forcing estimates from previous studies of sea spray geoengineering. Studies are categorized into either injected aerosol simulations or fixed cloud droplet number concentration (CDNC) simulations. The injected aerosol simulations are further divided into simulations that introduce sea spray aerosols in relation to the approximate mass fluxes suggested by the proposed design of *Salter et al.* [2008] (approximately 450 Tg total annual emissions), or simulations that increase background sea spray aerosol concentrations by a given factor. *Rap et al.* [2013] investigated removal of sea spray emissions from the present-day atmosphere. References for each data point are included in the legend.

Stephens, 2011], although the global net effect of these processes has a great deal of uncertainty [*Forster et al.*, 2007].

[4] Marine cloud brightening (MCB) relies on the radiative effects associated with aerosol-cloud interactions. In their assessment of geoengineering technologies, *Lenton and Vaughan* [2009] determined that, along with sunshades [e.g., *Angel*, 2006] and stratospheric sulfate aerosols [e.g., *Budyko*, 1974], MCB can potentially cause enough cooling to significantly offset warming from increasing levels of CO_2.

[5] Figure 1 shows a summary of the radiative effects from simulated MCB experiments that have been performed to date. Some of these experiments involve increases in CDNC, which approximates the end result of injecting sea spray aerosols into marine low clouds. Others involve direct emission of sea spray aerosols into the marine boundary layer. Therefore, in our discussion of all of these related experiments, we refer to them as sea spray geoengineering.

[6] *Rasch et al.* [2009] increased CDNC to $1000 \, cm^{-3}$ and found that of the chosen sea spray injection strategies they simulated, none could simultaneously restore global averages of temperature, precipitation, and sea ice from a 2xCO$_2$ climate (CO$_2$ concentrations were doubled from 335 ppm to 710 ppm) to an unperturbed climate state. *Jones et al.* [2009] increased CDNC from background levels (approximately $100 \, cm^{-3}$, ranging from 50 to $300 \, cm^{-3}$) to $375 \, cm^{-3}$ in three regions of permanent marine stratocumulus clouds and found

a very heterogeneous climate response. They also found that increasing CDNC in one particular region, in the South Atlantic off the coast of Africa, caused rainfall reduction over the Amazon, which was not found by *Rasch et al.* [2009] in a different model but has since been confirmed by *Latham et al.* [2012] using an earlier version of the same model as was used by *Jones et al.*, raising the question as to whether this response is model specific. *Korhonen et al.* [2010] found that achieving uniform CDNC of $375 \, cm^{-3}$ is likely impracticable, although *Partanen et al.* [2012], using a different model, showed that higher concentrations than those reported by *Korhonen et al.* could be achieved. There appears to be a strong dependence of achievable CDNC upon updraft velocity [*Pringle et al.*, 2012], in part explaining the much higher concentrations achieved by *Partanen et al.* In a different study, *Bala et al.* [2011] found that MCB did not substantially reduce precipitation over land, whereas solar reduction did. They also found that the global climate effects of MCB were dominated by large effects occurring in relatively small regions, supporting the results of *Jones et al.* [2010].

[7] Depending upon the injection strategy, the effective radiative forcing due to aerosol-radiation interactions (ERFari, also called the aerosol direct effect) can be equally important as those due to aerosol-cloud interactions (ERFaci, also called the aerosol indirect effects) [*Jones and Haywood*, 2012]. *Partanen et al.* [2012] found that ERFari accounted

Table 1. A Summary of the Three Sea Spray Geoengineering Experiments in This Paper[a]

Experiment	Description
G1ocean-albedo	Instantaneously quadruple the preindustrial CO_2 concentration while simultaneously increasing ocean albedo to counteract this forcing.
G4cdnc	In combination with RCP4.5 forcing, starting in 2021, increase cloud droplet number concentration by 50% over the ocean.
G4sea-salt	In combination with RCP4.5 forcing, starting in 2021, increase sea spray emissions in the marine boundary layer between 30°S and 30°N by a uniform amount, with an additional total flux of sea spray aerosols that results in a global-mean ERF of $-2.0\,\mathrm{W\,m^{-2}}$.

[a]Schematics of these experiments can be found in Figure 2. Each simulation is to be run for 50 years with sea spray geoengineering, followed by 20 years in which geoengineering is ceased. A 10 year fixed sea surface temperature experiment is also requested to diagnose ERF.

for 29% of the total radiative effect in their experimental setup. *Alterskjær et al.* [2012] found that due to a competition effect between the sea-salt aerosols and other particles, some injection strategies actually reverse the intended effects of MCB. *Wang et al.* [2011], *Jenkins et al.* [2012], and *Jenkins and Forster* [2013] found that the injection strategy is critical in affecting the spatial distribution of injected particles and the effectiveness of MCB under various boundary-layer meteorological conditions.

[8] These studies raised important questions regarding the expected climate effects of MCB, as well as the feasibility of reaching certain levels of CDNC and the consequent radiative changes. Although not an exhaustive list, we highlight several priorities in MCB research, several of which were suggested or inspired by *Latham et al.* [2008, 2012]:

[9] 1. To what degree will adding sea spray aerosols actually increase CCN and CDNC?

[10] 2. To what extent do the effects of MCB depend upon the location of clouds?

[11] 3. What are the relative strengths of aerosol–radiation and aerosol-cloud interactions through sea spray injection?

[12] 4. What is the expected climate response to sea spray geoengineering, particularly relating to land-sea temperature contrast and precipitation patterns?

[13] Previous climate and process modeling studies have made significant progress in understanding sea spray geoengineering and answering these questions, although most of the results are for individual models, and robust features of climate model response to sea spray geoengineering have not yet been established, if they exist. Coordinated modeling studies could reveal some of these robust features, particularly regarding the research questions listed above. Similar questions in stratospheric sulfate aerosol geoengineering were the impetus for the Geoengineering Model Intercomparison Project (GeoMIP), which defined four core experiments to be performed by all participating modeling groups [*Kravitz et al.*, 2011]. That effort has been quite successful in determining some of the robust climate model responses to idealized solar geoengineering [e.g., *Jones et al.*, 2013; *Kravitz et al.*, 2013; *Tilmes et al.*, 2013]. The Implications and Risks of Engineering Solar Radiation to Limit Climate Change (IMPLICC) project has performed a coordinated sea spray geoengineering experiment in three European

climate models. Our intent here is to take a similar approach and use the larger GeoMIP framework to generate a broader set of sea spray geoengineering simulations.

[14] One concern not explicitly addressed in the following proposed experiments is identification of which regions would most likely be targeted in real world deployment of MCB. In particular, enhancement of cloud albedo via sea spray injection will be most effective in regions containing persistent low-level clouds in relatively pristine marine environments. Previous modeling studies have highlighted the marine stratocumulus decks off the West coasts of North America, tropical South America, and Southwest Africa as the most susceptible to brightening [e.g., *Latham et al.*, 2008; *Jones et al.*, 2009; *Rasch et al.*, 2009; *Jones and Haywood*, 2012; *Partanen et al.*, 2012]. *Alterskjær et al.* [2012] found that their model shows higher susceptibility in
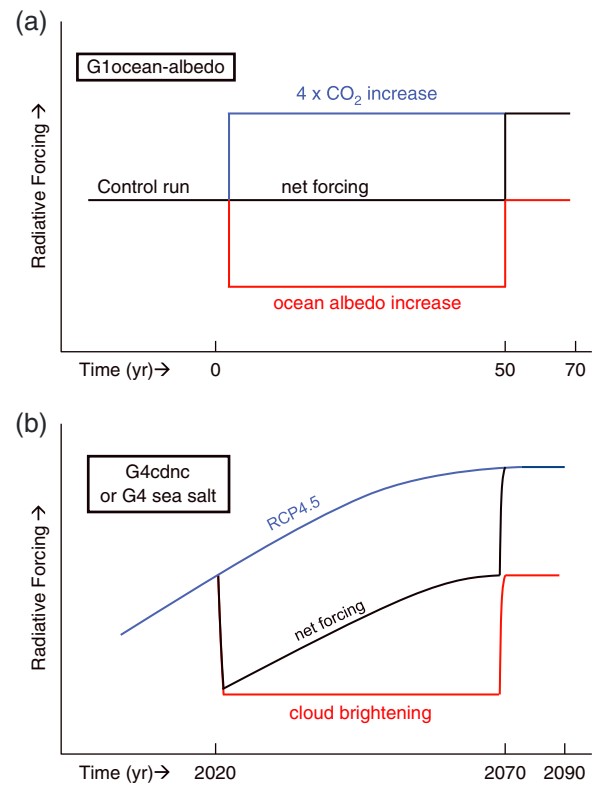

Figure 2. Schematics of the three experiments outlined in this paper. (Top) *G1ocean-albedo* is started from a stable preindustrial control run; an instantaneous quadrupling of CO_2 concentrations is balanced by an increase in ocean albedo. (Bottom) *G4cdnc* and *G4sea-salt* are started from year 2020 in an RCP4.5 scenario; the radiative forcing from RCP4.5 is partially offset by a constant level of geoengineering via marine cloud brightening. In these two experiments, we do not set a goal of achieving top-of-atmosphere radiative flux balance. In *G4cdnc*, cloud droplet number concentration in marine low clouds is increased by 50%. In *G4sea-salt*, sea spray is injected into the marine boundary layer to achieve a global-mean ERF of $-2.0\,\mathrm{W\,m^{-2}}$. All three experiments are run with geoengineering for 50 years, followed by 20 years of cessation of geoengineering. This figure illustrates experimental design and is not intended to accurately represent emergent behavior resulting from feedbacks.

slightly different regions; their identified regions show good agreement with a susceptibility index obtained from MODIS retrievals. Additionally, *Rosenfeld et al.* [2008] have shown that the sensitivity of cloud albedo increase and precipitation suppression in marine low clouds is reduced in polluted regions. Adding an additional level of complication, large sea-salt particles acting as CCN can increase rain and thus scavenge pollution particles, cleansing the air and reducing the effects of pollution [*Rosenfeld et al.*, 2002; *Rudich et al.*, 2002]. Further study of the regions most susceptible to cloud brightening is warranted. To avoid prescription of any particular strategy of MCB implementation, as well as potential mismatches between different models' representations of the most susceptible regions, our proposed experiments do not target any particular region of persistent low clouds.

[15] In the following sections, we outline three core experiments of varying complexity representing sea spray geoengineering to be conducted under the GeoMIP framework. Table 1 and Figure 2 outline the designs of these three experiments, which are described below. We also present preliminary results from individual climate models which demonstrate the feasibility of the designed experiments in addressing various aspects of the four research questions listed above, and we suggest ways in which conducting these experiments under the framework of GeoMIP would enhance scientific understanding.

[16] We promote the recommendation of *Jones et al.* [2009] that the effective radiative forcing (ERF) be used to characterize the strength of the forcing instead of radiative forcing [*Hansen et al.*, 2005]. ERF, also previously called radiative flux perturbation [*Haywood et al.*, 2009], is now a commonly reported metric that estimates the changes in net top-of-atmosphere radiative fluxes between two fixed-sea surface temperature (SST) experiments. This is justified by the fact that the radiative forcing concept does not fully account for all adjustments associated with aerosol-cloud interactions (particularly the cloud lifetime effect), which form an essential part of MCB. Use of the concept of ERF will therefore be particularly relevant for the *G4sea-salt* experiment (section 2.3 below).

[17] For the original GeoMIP experiments, forcing was applied at the top of the atmosphere or in the stratosphere. Thus, it was simple for all models to apply the forcing in the same manner and with similar spatial patterns. For the sea spray geoengineering experiments proposed here, we expect the forcing to exhibit more intermodel differences, which may complicate the interpretation of the different climate responses.

2. Description of Experimental Design

[18] We outline below three experiments representing various aspects of sea spray geoengineering of varying complexity. *G1ocean-albedo* (section 2.1) is the simplest experiment, involving an increase in ocean albedo. It is designed to minimize geographical heterogeneity of the applied forcing, as well as be independent of cloud microphysical parameterizations. *G4cdnc* (section 2.2) is a more complicated experiment. It operates on the assumption that clouds can be brightened, prescribing an increase in CDNC in all liquid clouds. *G4sea-salt* (section 2.3), arguably the most

physically based of the three experiments, tests the ability of sea spray injection into the marine boundary layer to achieve a radiative forcing that would offset radiative forcing from increased CO_2 concentrations.

[19] Experiment *G1ocean-albedo* is to begin from a stable preindustrial climate. In this experiment, sea spray geoengineering will be used to balance the radiative forcing due to an abrupt quadrupling of CO_2 concentrations. Experiments *G4cdnc* and *G4sea-salt* begin in the year 2021 of an RCP4.5 scenario [*Taylor et al.*, 2012]. These simulations involve a prescribed constant amount of geoengineering which will partially offset the climate prescribed by an RCP4.5 scenario. Figure 2 gives a schematic of these three experiments, which are described in more detail below.

[20] To address the calculation of ERF, we propose that each experiment below be conducted using two setups. One set of simulations involves three ensemble members of fully coupled atmosphere-ocean simulations in which solar geoengineering is performed for 50 years. After 50 years, solar geoengineering is to be abruptly ceased, and the experiment is to be run for an additional 20 years to assess the termination effect [e.g., *Wigley*, 2006; *Jones et al.*, 2013]. Another set should be conducted as a single 10 year simulation with fixed sea surface temperatures and sea ice. This will aid in diagnosing the ERF associated with the experiments.

[21] In this section and section 3, we present results from experiments *G1ocean-albedo* and *G4sea-salt*. We do not include results from experiment *G4cdnc*, as multiple previous studies include similar experiments [e.g., *Jones et al.*, 2009; *Rasch et al.*, 2009; *Bala et al.*, 2011; *Latham et al.*, 2012], and presenting results from additional single-model studies would not add clarity to the experimental design.

2.1. Experiment G1ocean-Albedo

[22] This experiment is designed following GeoMIP experiment *G1* [*Kravitz et al.*, 2011], in which a uniform insolation reduction is used to counteract the radiative forcing from an abrupt quadrupling of CO_2 concentrations from preindustrial levels. In *G1ocean-albedo*, the net top-of-atmosphere radiative flux imbalance due to an abrupt quadrupling of CO_2 concentrations is offset by an increase in ocean surface albedo. The purpose of this experiment is to provide an idealized way of representing a generic MCB-like albedo change in climate models with minimal intermodel diversity in representing the applied forcing. In particular, the forcing is prescribed in similar locations in all models, simulating some of the effects of MCB or, more generally, sea spray geoengineering. This experiment will serve as an idealized way of evaluating changes in circulation due to changes in the land-sea contrast of temperature changes; the results presented in section 3 suggest land-sea contrast will be an important feature of MCB experiments. Although this experiment minimizes geographical inhomogeneity of the applied forcing, the net forcing will be less in cloudy regions. The differences in ERF simulated by the GeoMIP models will be a measure of the differences in how clouds affect the impact of a surface albedo change among these models. This experiment can be performed by all models, independent of the complexity of each model's cloud microphysical parameterization.
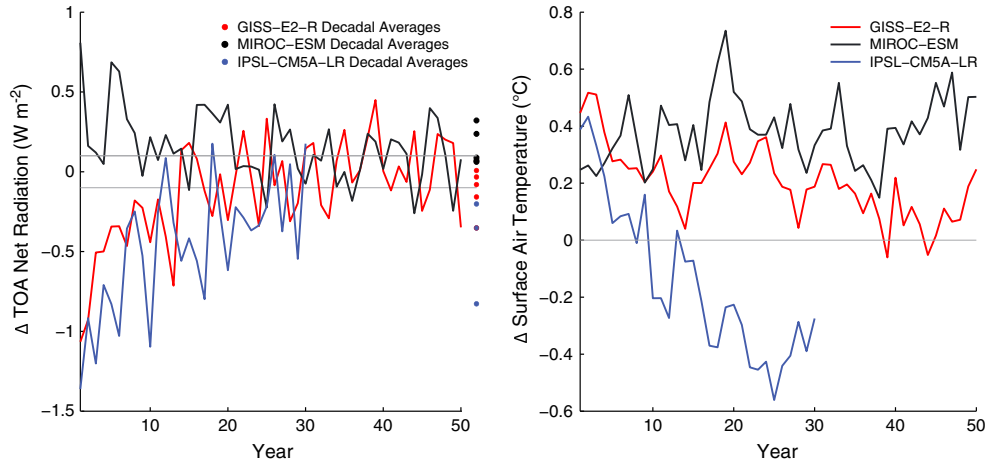
Figure 3. Globally averaged top-of-atmosphere net radiation and temperature changes (from preindustrial) simulations of *G1ocean-albedo* with GISS-E2-R (red), MIROC-ESM (black), and IPSL-CM5A-LR (blue). Grey lines in the left panel show the specified $\pm 0.1 \, W \, m^{-2}$ range for compensating radiation changes due to increased CO_2 concentrations. Dots in the left panel show decadal averages. GISS-E2-R and MIROC-ESM were run for 50 years and show results from simulations that have achieved radiative balance to the specifications of the experiment. IPSL-CM5A-LR was run for 30 years and has not yet achieved radiative balance.

[23] Beginning from a stable preindustrial control run, if α is the value of the ocean albedo in a given grid box (where α is a fraction of 1), the new ocean albedo in that grid box will be set to α' = min(δα, 1.0), where δ is a constant for all model radiative bands in the shortwave spectrum. This multiplicative constant δ should be applied in all oceanic grid boxes and in the oceanic part of grid boxes also containing sea ice or land. The sea ice albedo itself should not be changed. In the case where the ocean is modeled as a non-Lambertian surface, this method should not affect the angular dependency in the parameterized surface reflectance, and should be applied uniformly in all directions. However, the resulting surface albedo should also be capped to a maximum value of 1.0. The constant δ is applied uniformly in space and time in a given model but will vary across models.

[24] In the original *G1* experiment [*Kravitz et al.*, 2011], "compensation" for radiative flux imbalance meant that the net radiation balance at the top of atmosphere was to be less than $0.1 \, W \, m^{-2}$ in the global mean as an average over the first 10 years of simulation. However, Figure 3 shows that the first 10 years of simulation involves adjustments due to climate system feedbacks; thus, quasi-equilibrium has not yet been reached by the end of 10 years. Based on the results in Figure 3, which were conducted using GISS ModelE2 [*Schmidt et al.*, 2006], MIROC-ESM [*Watanabe et al.*, 2011], and IPSL-CM5A-LR [*Dufresne et al.*, 2013], analysis of an average over years 21–30 of the simulation is required to determine whether the compensation is within $0.1 \, W \, m^{-2}$ of preindustrial levels (i.e., between the grey lines in Figure 3). As such, we define "compensation" in this experiment to mean that top-of-atmosphere radiative flux imbalance is within $0.1 \, W \, m^{-2}$ of preindustrial levels in the decadal average over years 21–30.

[25] The results in Figure 3 required an increase in ocean albedo in each grid box of 153% ($\delta = 2.53$) for GISS-E2-R, 150% ($\delta = 2.50$) for MIROC-ESM, and 140% ($\delta = 2.40$) for IPSL-CM5A-LR. The values for GISS-E2-R and MIROC-

ESM were obtained by performing two test simulations in which the ocean albedo was increased by different amounts. The appropriate amount of albedo increase was then estimated via linear interpolation or extrapolation. This method, although conceptually simplistic, results in obtaining the level of albedo increase that results in top-of-atmosphere radiative flux balance for the decadal average of years 21–30. In this experiment, globally averaged temperatures do not return to preindustrial levels in GISS-E2-R until approximately year 40, and they do not return to preindustrial values at all in MIROC-ESM. The chosen value of δ for IPSL-CM5A-LR is too high, resulting in a negative top-of-atmosphere radiative flux imbalance in the third decade of simulation (this simulation was ceased after 30 years), as well as substantial cooling over the course of the simulation.

[26] We have not yet determined the reason for this lag in achieving compensation, nor the reason for the disparity between top-of-atmosphere radiative balance and a temperature change from the preindustrial era. Further tests exploring these details could yield clues about strengths of climate system feedbacks.

2.2. Experiment G4cdnc

[27] This experiment is based on GeoMIP experiment *G4* [*Kravitz et al.*, 2011], in which the radiative forcing from an RCP4.5 scenario is partially offset by a constant level of solar geoengineering. In *G4cdnc*, solar geoengineering is represented by an increase in cloud droplet number concentration (CDNC) in marine low-level clouds. The purpose of this experiment is to identify the effects of MCB under the assumption that a 50% increase in CDNC can be achieved in marine clouds, an approach similar to that of *Jones et al.* [2009]. In particular, this experiment is well suited to determine a question posed by *Bala et al.* [2011], reiterated in question #2 of section 1, which is whether the results of MCB depend upon the locations of clouds. The following
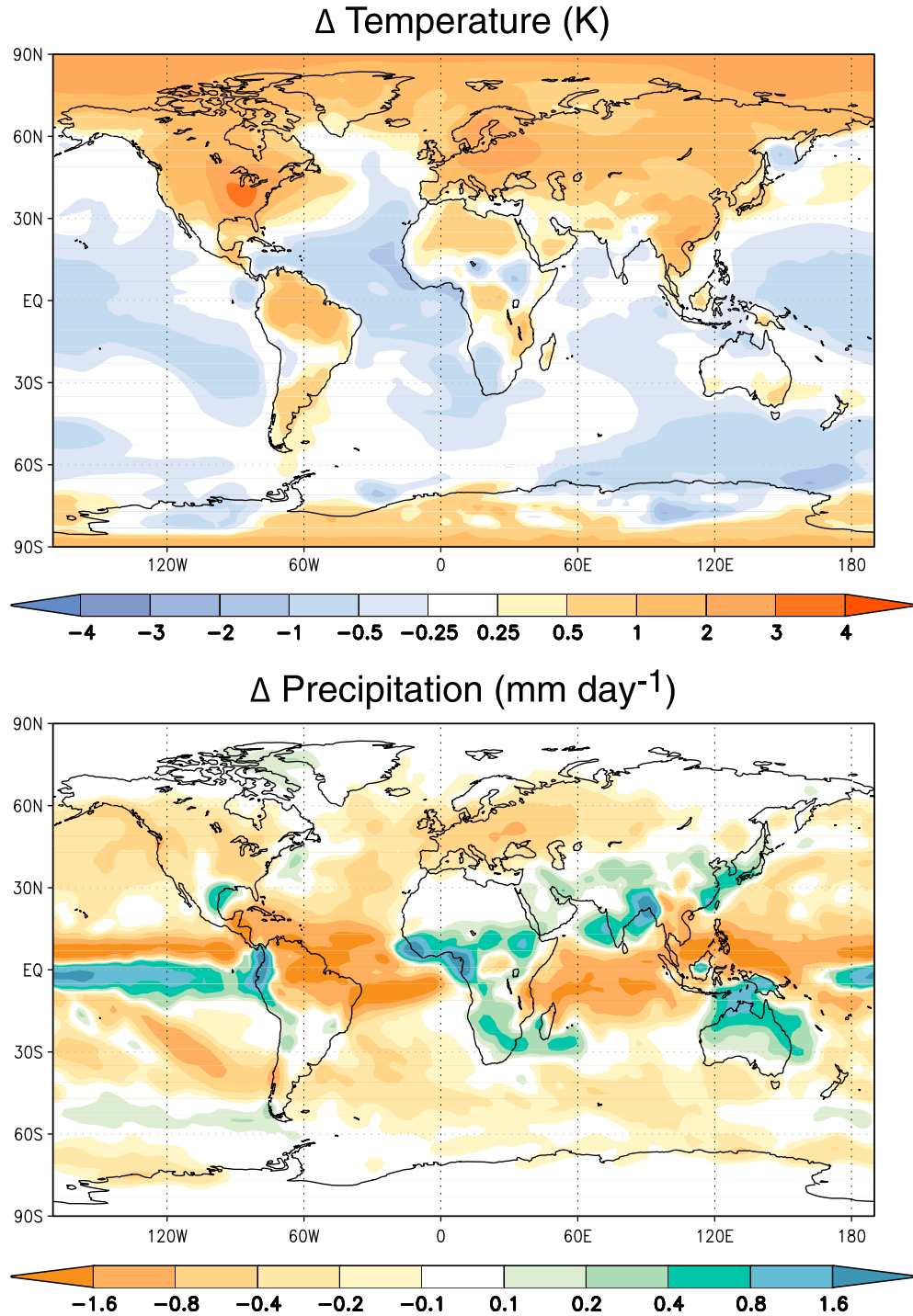
Δ Temperature (K)

Δ Precipitation (mm day^{-1})

Figure 4. Temperature (K) and precipitation (mm d^{-1}) changes (from preindustrial) for the GISS ModelE2 simulations of *G1ocean-albedo*. All values shown are averages over years 41–50 of simulation.

experiment, *G4sea-salt*, includes aerosol microphysical parameterizations and will give an indication as to whether the concentrations specified by *G4cdnc* can actually be achieved. Also, *G4cdnc* discounts any potential aerosol-radiation interactions that would be realized from direct sea spray injection. These aerosol-radiation interactions will be included in experiment *G4sea-salt*.

[28] Performing this experiment in a multimodel setting has two primary goals. The first is to determine the range of radiative perturbations that are associated with increasing CDNC in the manner described above. The second is to determine what robust features, if any, emerge for increasing CDNC in models with different distributions of clouds. Clouds are known to be the largest source of intermodel variability in determining the hydrological cycle response to increased CO_2 [*Allen and Ingram*, 2002]. A GeoMIP-like framework is essential for characterizing and resolving some of these uncertainties.
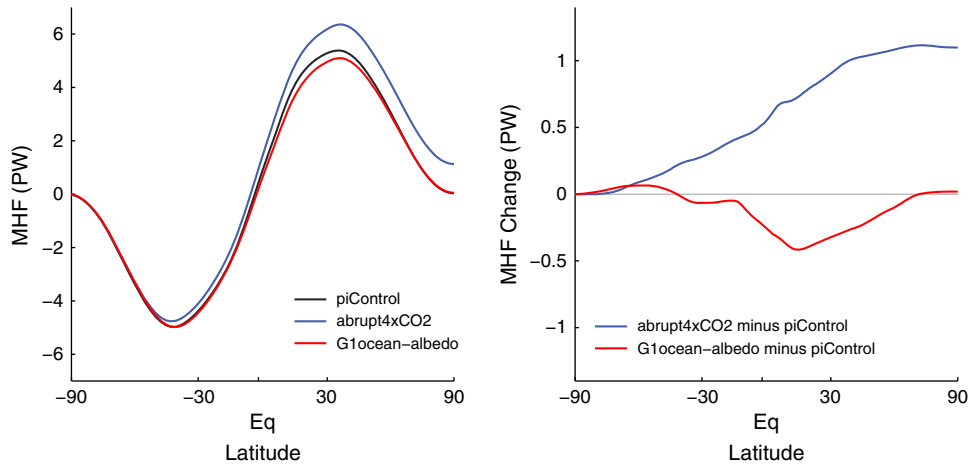
Figure 5. Changes in total (atmospheric + oceanic) meridional heat flux (MHF), measured in PW, for the experiments discussed in section 2. All simulations were conducted using GISS ModelE2. Calculations of MHF were performed using the method of *Wunsch* [2005] over an average of years 41–50 of simulation. Values at each latitude in the left panel are a cumulative sum of latitude-weighted fluxes from 90°S to that latitude; the final sum at 90°N is defined as the MHF. *piControl* indicates a preindustrial control simulation, *abrupt4xCO2* indicates a simulation in which CO_2 concentrations were instantaneously quadrupled from the preindustrial era, and *G1ocean-albedo* is the simulation described in section 2.

[29] In *G4cdnc*, all liquid cloud droplets over ocean regions and at an altitude below 680 hPa will be identified during each model time step of the simulation. This includes droplets in pure liquid-phase clouds and liquid droplets in mixed-phase clouds. In these clouds, CDNC is to be increased uniformly by 50% as compared to what it would have been without MCB. In prognostic aerosol schemes, a memory of the unperturbed CDNC state will need to be maintained throughout the simulation. To properly include the associated feedbacks, no direct alterations of cloud droplet size and cloud water content are to be prescribed by this experiment protocol. However, cloud droplet size and water content will respond to the change in CDNC, allowing for more spatial and temporal inhomogeneity and more diverse representation of potential cloud albedo enhancement in the various models than in the *G1ocean-albedo* experiment. For grid boxes that contain coastline, the percentage increase in CDNC should be multiplied by the ocean fraction *f* for these grid boxes, namely,

$$CDNC' = (1 + 0.5f)CDNC$$

[30] If the model has separate CDNC specifications in the radiation and cloud microphysics routines, CDNC should be increased in both places, which will represent both the cloud albedo and cloud lifetime effects as well as associated rapid adjustment and feedbacks.

2.3. Experiment G4sea-Salt

[31] *G4sea-salt* is also based on GeoMIP experiment *G4* but adds a level of complexity as compared to *G4cdnc*. In *G4sea-salt*, solar geoengineering is represented by a constant rate of injection of sea spray aerosols into the tropical marine boundary layer to achieve a global-mean ERF of $-2.0\,\mathrm{W\,m^{-2}}$. This simulation is the most complicated in the suite and will reveal numerous features of sea spray geoengineering, including the

model dependence in predicting CDNC and its changes because of differences in the treatment of updraft velocity, aerosol activation, and cloud microphysics, as well as inclusion of aerosol-radiation interactions of the injected sea spray aerosols.

[32] Using its own aerosol and cloud microphysical parameterizations for the aerosol-cloud interactions (to participate in *G4sea-salt*, models should have a treatment of these processes), each model should inject an amount of sea spray per year into the boundary layer uniformly over oceans and contained between 30°S and 30°N such that the generated ERF (ERFari + ERFaci) is $-2.0 \pm 0.1\,\mathrm{W\,m^{-2}}$. The oceanic regions between 30°S and 30°N have been identified as containing most of the radiatively important stratocumulus cloud decks [*Alterskjær et al.*, 2012; *Jones and Haywood*, 2012]. Injection should be performed as frequently as the model allows. We only specify that injection should be into the marine boundary layer; we do not specify the injection height, as each model will handle this specification in accordance with its respective sea spray representation. For models that have multiple modes or options representing sea spray aerosols, the new particles should have a size corresponding to the accumulation mode. *Alterskjær and Kristjánsson* [2013] showed that injection of particles into this mode results in a negative radiative forcing, whereas particles injected into the Aitken or coarse modes may cause a positive forcing, as was the case in their model. This experiment would be expected to show the most diversity of results of all three experiments.

[33] In general, ERF would not be expected to scale linearly with sea-salt emission across the entire range of possible emissions rates [Figure 1; *Korhonen et al.*, 2010]. However, as will be discussed in the following section, preliminary simulations indicate that globally averaged ERF is approximately linear with sea-salt emissions rate within an emissions range that includes the desired ERF of $-2.0\,\mathrm{W\,m^{-2}}$. Therefore, determining the proper amount of aerosol injection in *G4sea-salt* can be accomplished via linear interpolation/extrapolation between two 10 year test simulations.
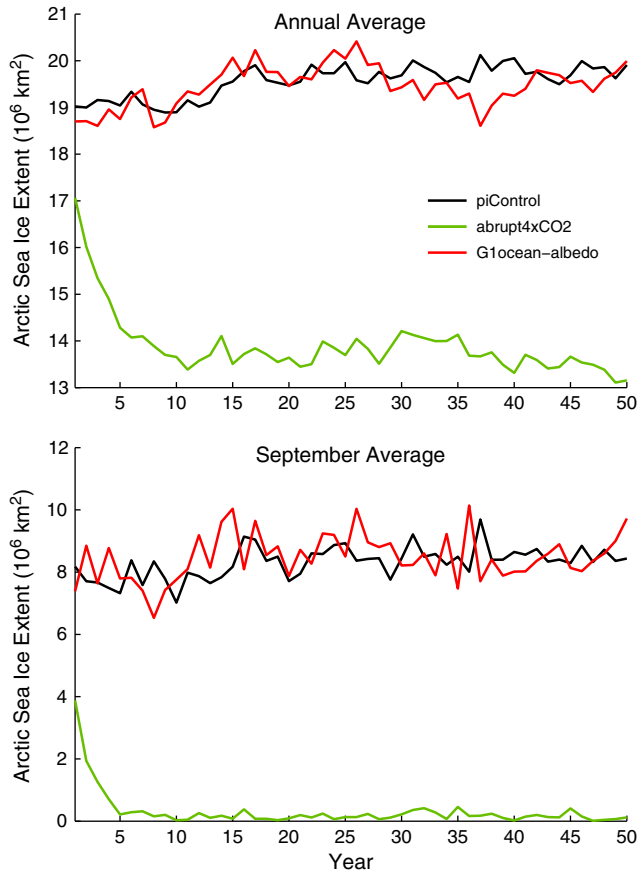
Figure 6. (Top) Annually averaged and (bottom) September Arctic sea ice extent simulated using GISS ModelE2. *piControl* indicates a preindustrial control simulation, *abrupt4xCO2* indicates a simulation in which CO_2 concentrations were instantaneously quadrupled from the preindustrial era, and *G1ocean-albedo* is the simulation described in section 2.

3. Preliminary Results and Discussion

[34] Figure 4 shows temperature and precipitation changes for an average of years 41–50 of the *G1ocean-albedo* simulation using GISS ModelE2. The results of this experiment are more spatially inhomogeneous than *G1*, which supplied a uniform solar reduction [*Kravitz et al.*, 2013]. In particular, despite global-mean temperature differences from preindustrial being −0.08 K over years 41–50, land temperatures show an increase by 0.15 K, whereas ocean temperatures in the tropics and midlatitudes (66.55°S to 66.55°N) show a decrease in temperature of 0.20 K. The Arctic (areas North of 66.55°N) shows an increase in temperature of 0.32 K, which is lower than the residual temperature increase of 0.81 K found by *Kravitz et al.* [2013] for experiment *G1*. The precipitation results also show spatial inhomogeneity, with significant shifts in the Intertropical Convergence Zone. The precipitation changes in the tropical Pacific are similar to those of the 70PCT experiment of *Rasch et al.* [2009]. Parts of India, Australia, and the Sahel show increases in precipitation exceeding 1 mm d^{-1}. Most of the ocean shows a decrease in precipitation, as do the midlatitude storm tracks. Obtaining similar results in other models will increase our confidence in these conclusions.

[35] Figure 4 also shows that the Arctic still shows warming by 0.32 K. *Parkes et al.* [2012] showed that MCB significantly reduces the total (atmosphere + ocean) meridional heat flux (MHF). Figure 5 shows MHF results for *G1ocean-albedo*, compared to a preindustrial control experiment and an experiment in which CO_2 concentrations were abruptly quadrupled. MHF calculations were performed using the method of *Wunsch* [2005]. *G1ocean-albedo* also reduces MHF, consistent with *Parkes et al.* [2012], approximately to preindustrial levels. Although it is difficult to determine the relationship between MHF slowdown and Arctic temperatures, results from ModelE2 do not provide evidence that the Arctic warming is due to changes in annual mean heat flux. Instead, the Arctic warming could be due to changes in the seasonal cycle or local changes in albedo or forcing [*Crook et al.*, 2011; *Crook and Forster*, 2011]. *Crook et al.* [2011] showed that the role of MHF change in influencing Arctic warming varied across models. As such, performing this experiment across a range of models will help determine whether these precipitation and MHF changes are from robust circulation changes that result from a change in the land-sea contrast of albedo.

[36] Figure 6 shows changes in annually averaged Arctic sea ice extent for *G1ocean-albedo*. As shown by *Kravitz et al.* [2013], an abrupt quadrupling of CO_2 causes a reduction in Arctic sea ice extent reaching −6.75 million km^2 in year 50 of the simulation. *G1* is capable of reducing this loss to −0.19 million km^2. *G1ocean-albedo* is also capable of preventing sea ice loss, with a residual change (average over years 41–50) of −0.11 million km^2. Minimum Arctic sea ice extent is often determined by analysis of September sea ice coverage; the Arctic becomes ice free in September in *abrupt4xCO2*, but *G1ocean-albedo* maintains September sea ice extent near preindustrial levels. The sea ice extent time series of *G1ocean-albedo* matches the time series of the preindustrial control run, whereas the top-of-atmosphere net radiation and temperature time series (Figure 3) show a separation for several decades. Because sea ice extent in *G1ocean-albedo* shows little change from the preindustrial control experiment, we are as of yet unable to determine the mechanisms that cause the residual Arctic warming seen in Figure 4.

[37] As stated previously, *Jones et al.* [2009] and *Latham et al.* [2012] found reductions in Amazon precipitation, whereas *Rasch et al.* [2009] did not. Figure 4 shows a reduction in Amazon precipitation, despite no direct modification of CDNC, suggesting these results are features of changing circulation patterns. A multimodel intercomparison will be necessary for and quite effective at determining changes in circulation patterns, as well as potential impacts due to the location or absence of clouds, in causing precipitation changes.

[38] Figures 7 and 8 show changes in CDNC and ERF, respectively, following the *G4sea-salt* protocol simulated by the HadGEM2-ES model [*Collins et al.*, 2011]. A sea spray injection rate of 100 Tg a^{-1} (dry sea-salt aerosol) results in a modest increase in CDNC in regions containing clouds (Figure 7), at least one order of magnitude lower than the values prescribed by *Jones et al.* [2009]. Thus, given the experimental protocol, the effects from aerosol-radiation interactions would be expected to be stronger than effects due to aerosol-cloud interactions.

[39] Figure 8 shows that this injection rate creates a globally averaged top-of-atmosphere net ERF of −1.1 W m^{-2}. Figure 9 shows that linearity in a range of ERF values around
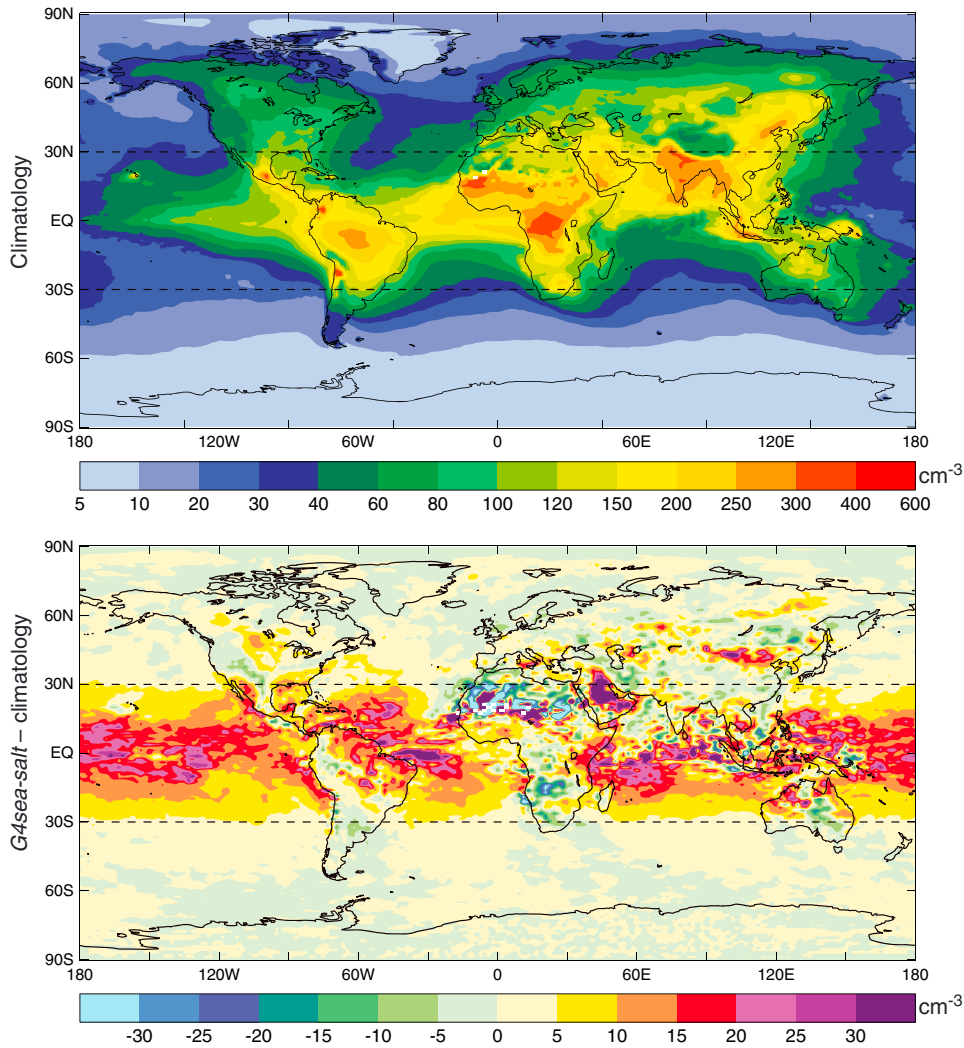
Figure 7. Ten year mean CDNC simulated by HadGEM2-ES for experiment *G4sea-salt*. All values shown are averages over the altitude range 500–1500 m. Top panel shows climatology of unperturbed CDNC, and bottom panel shows CDNC differences (*G4sea-salt* minus climatology). Global-mean CDNC in the top panel is 75.1 cm^{-3}, and 30°S to 30°N mean is 107.8 cm^{-3}. Changes in the bottom panel are 5.0 cm^{-3} and 9.1 cm^{-3} for the global mean and 30°S–30°N mean, respectively.

-2.0 W m^{-2} is a reasonable assumption. Also, because the intercept of Figure 9 associated with no injection is nonzero, this figure does indicate some degree of nonlinearity. Assuming linearity with mass loading based on the results in Figure 9, achieving an ERF of -2.0 W m^{-2} would require an injection rate of approximately 212 Tg a^{-1} in HadGEM2-ES. For comparison, the net ERF in HadGEM2-ES in experiment *G4* is -1.4 W m^{-2}. *Alterskjær et al.* [2012] injected sea spray on the order of 11,000 Tg a^{-1} over all open ocean and obtained a globally averaged radiative forcing of -4.8 W m^{-2}. Aerosol-radiation interactions were not included in this estimate, and the ERF includes only the contribution from aerosol-cloud interactions. Comparing these two values is difficult, as linearity with the amount of injection does not hold in general (although approximate linearity appears to be a good assumption for emission of accumulation mode aerosols of an amount that will yield values of ERF at or near -2.0 W m^{-2}), and the quantity reported in Figure 8 is ERF, rather than radiative forcing. Simulating injection over the same region (oceans between 30°S and 30°N) in three different models to offset an RF of ~1.5 W m^2 required injection rates of 266, 316, and 560 Tg a^{-1} (*K. Alterskjær*, personal communication).

[40] The largest ERF values in Figure 8 are generally confined to within the 30°S to 30°N injection area, which is consistent with a low atmospheric lifetime of marine boundary layer sea salt. Although the purpose of sea spray injection is to enhance aerosol-cloud interactions, further simulations with HadGEM2-ES to isolate the contributions of aerosol-radiation interactions and aerosol-cloud interactions indicate that the ERF from the aerosol-cloud interactions is approximately -0.4 W m^2 and that due to the aerosol-radiation interactions is larger at -0.7 W m^{-2}. Because aerosol was injected over the entire marine region between 30°S and 30°N, instead of only injecting into regions with clouds, aerosol-radiation interactions were enhanced over cloud-free regions, increasing the albedo over those regions from values which correspond to a dark ocean surface.
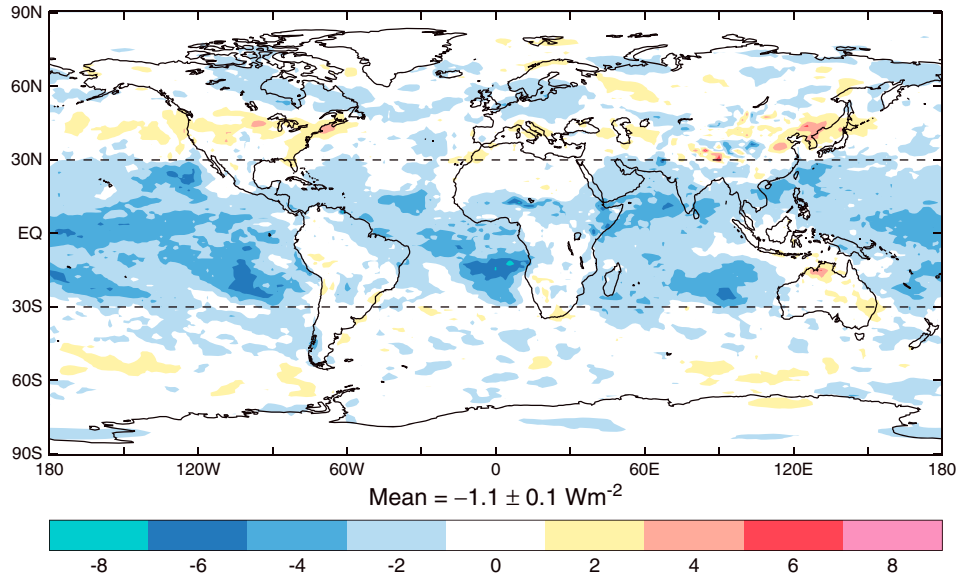
Figure 8. Ten year mean effective radiative forcing in *G4sea-salt* simulated by HadGEM2-ES in response to a sea spray injection rate equivalent 100 Tg dry sea salt a^{-1} in the accumulation mode.

[41] As in previous experiments, analysis of the land-sea temperature contrast will be a primary focus of the multimodel analysis of *G4sea-salt*. Determining the net effects, the range of model responses, and the resulting patterns of CDNC changes will be other useful objectives.
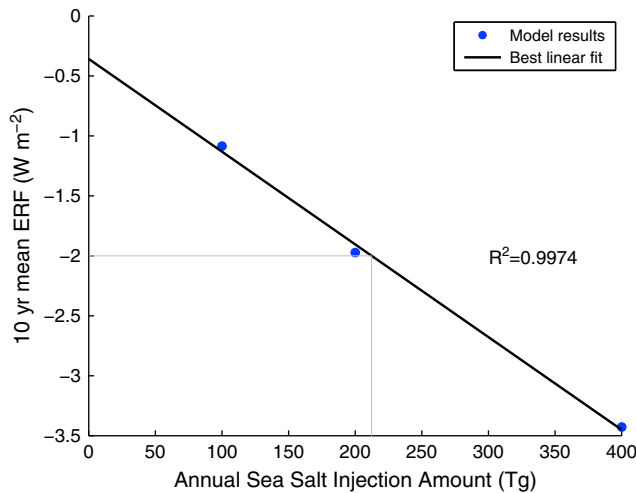

Figure 9. Illustration of the linearity of ERF (ordinate; W m^{-2}) with respect to annual sea spray emissions rate (abscissa; Tg dry sea salt a^{-1}) for experiment *G4sea-salt*. Three simulations with different sea spray emissions rates were performed using HadGEM2-ES. The best fit line was calculated using ordinary least squares regression on the three plotted points. Linear interpolation gives an annual emissions rate of 212 Tg dry sea salt a^{-1} to achieve an ERF of -2.0 W m^{-2} (grey lines). The nonzero ordinate intercept (-0.35 W m^{-2}) indicates some degree of nonlinearity with injection rate, but linearity is a good approximation in the neighborhood of -2.0 W m^{-2}.

4. Conclusions

[42] Preliminary results show that sea spray geoengineering, as simulated in the three experiments described previously, can be effective at offsetting some amount of forcing from anthropogenic climate change. The land-sea temperature contrast is likely to change significantly in all experiments. The change in CDNC specified in *G4cdnc* is not necessarily attainable in the real world, as it depends upon meteorology and microphysics that vary across models. The issues raised here, including the four research directions outlined in section 1, will strongly benefit from a multimodel intercomparison.

[43] The experiments proposed here are global in scale and aim to examine global and large regional scale responses to cloud brightening. They do not address the engineering concerns mentioned by *Latham et al.* [2008, 2012], such as how such large amounts of sea water can be injected into the marine boundary layer. Although there are theoretical proposals for ships to inject sea water into the atmosphere [e.g., *Salter et al.*, 2008], none have been built, and it is yet to be demonstrated that the particles can be lofted into boundary layer clouds or that they can generate more, smaller cloud droplets. Furthermore, the effectiveness of sea spray geoengineering depends upon the meteorological and background conditions [*Wang et al.*, 2011; *Jenkins et al.*, 2012]. Small-scale circulation may produce subsidence next to the areas of aerosol injection and overall impacts in the opposite direction to that which is intended [e.g., *Wang et al.*, 2011]. Fine-resolution modeling studies [e.g., *Wang and Feingold*, 2009a, 2009b] have revealed complex microphysical and dynamical responses of marine stratocumulus clouds to aerosol perturbations that can modify local cloud albedo, perhaps more complicated than can be represented in many general circulation models. More such high-resolution studies are needed to determine the dependence of cloud changes on the specific circumstances of the injections, including the pattern of injection and the cellular nature of the cloud fields.

[44] The experiments proposed here assume that large-scale MCB is possible, but whether this is the case remains to be seen. The purpose of this paper is not to advocate field experiments to determine the possibility of MCB. Any legitimate potential experiments would need to be subjected to rigorous, transparent environmental impact analyses and governance; such a framework does not currently exist.

[45] Further details regarding these experiments, as well as progress on their simulation by various modeling groups, will be available on the GeoMIP website: http://climate.envsci.rutgers.edu/GeoMIP/.

References

Albrecht, B. A. (1989), Aerosols, cloud microphysics, and fractional cloudiness, *Science*, *245*(4923), 1227–1230, doi:10.1126/science.245.4923.1227.

Allen, M. R., and W. J. Ingram (2002), Constraints on future changes in climate and the hydrological cycle, *Nature*, *419*, 223–232.

Alterskjær, K., and J. E. Kristjánsson (2013), The sign of the radiative forcing from marine cloud brightening depends on both particle size and injection amount, *Geophys. Res. Lett.*, *40*, 210–215, doi:10.1029/2012GL054286.

Alterskjær, K., J. E. Kristjánsson, and Ø. Seland (2012), Sensitivity to deliberate sea salt seeding of marine clouds – Observations and model simulations, *Atmos. Chem. Phys.*, *12*, 2795–2807, doi:10.5194/acp-12-2795-2012.

Angel, R. (2006), Feasibility of cooling the Earth with a cloud of small spacecraft near the inner Lagrange point (L1), *Proc. Natl. Acad. Sci. U. S. A.*, *103*, 17,184–17,189.

Bala, G., K. Caldeira, R. Nemani, L. Cao, G. Ban-Weiss, and H.-J. Shin (2011), Albedo enhancement of marine clouds to counteract global warming: Impacts on the hydrological cycle, *Clim. Dyn.*, *37*, 915–931, doi:10.1007/s00382-010-0868-1.

Budyko, M. I. (1974), *Climate and life*, Academic Press, New York, pp. 508.

Christensen, M. W., and G. L. Stephens (2011), Microphysical and macrophysical responses of marine stratocumulus polluted by underlying ships: Evidence of cloud deepening, *J. Geophys. Res.*, *116*, D03201, doi:10.1029/2010JD014638.

Collins, W. J., et al. (2011), Development and evaluation of an Earth-System model—HadGEM2, *Geosci. Model Dev.*, *4*, 1051–1075, doi:10.5194/gmd-4-1051-2011.

Crook, J. A., and P. M. Forster (2011), A balance between radiative forcing and climate feedback in the modeled 20th century temperature response, *J. Geophys. Res.*, *116*, D17108, doi:10.1029/2011JD015924.

Crook, J. A., P. M. Forster, and N. Stuber (2011), Spatial patterns of modeled climate feedback and contributions to temperature response and polar amplification, *J. Clim.*, *24*, 3575–3592.

Crutzen, P. J. (2006), Albedo enhancement by stratospheric sulfur injections: A contribution to resolve a policy dilemma?, *Clim. Change*, *77*(3–4), 211–220, doi:10.1007/s10584-006-9101-y.

Dufresne, J.-L., et al. (2013), Climate change projections using the IPSL-CM5 Earth System Model: From CMIP3 to CMIP5, *Clim. Dyn.*, *40*, 2123–2165, doi:10.1007/s00382-012-1636-1.

Forster, P. M., et al. (2007), Changes in atmospheric constituents and in radiative forcing, in *Climate Change 2007: The Physical Science Basis. Contribution of Working Group I to the Fourth Assessment Report of the Intergovernmental Panel on Climate Change* [Solomon, S., D. Qin, M. Manning, Z. Chen, M. Marquis, K. B. Averyt, M. Tignor, and H. L. Miller (eds.)]. Cambridge University Press, Cambridge, United Kingdom and New York, NY, USA.

Hansen, J., et al. (2005), Efficacy of climate forcings, *J. Geophys. Res.*, *110*, D18104, doi:10.1029/2005JD005776.

Haywood, J., L. J. Donner, A. Jones, and J.-C. Golaz (2009), Global indirect radiative forcing caused by aerosols: IPCC (2007) and beyond, in *Clouds in the Perturbed Climate System*, edited by J. Heintzenberg and R. J. Charlson, pp. 451–467, MIT Press, Cambridge.

Hill, S., and Y. Ming (2012), Nonlinear climate response to regional brightening of tropical marine stratocumulus, *Geophys. Res. Lett.*, *39*, L15707, doi:10.1029/2012GL052064.

Jenkins, A. K. L., and P. M. Forster (2013), The inclusion of water with the injected aerosol reduces the simulated effectiveness of marine cloud brightening, *Atmos. Sci. Lett.*, *14*(3), 164–169, doi:10.1002/asl2.434.

Jenkins, A. K. L., P. M. Forster, and L. S. Jackson (2012), The effects of timing and rate of marine cloud brightening aerosol injection on albedo changes during the diurnal cycle of marine stratocumulus clouds, *Atmos. Chem. Phys.*, *13*, 1659–1673, doi:10.5194/acp-13-1659-2013.

Jones, A., and J. M. Haywood (2012), Sea-spray geoengineering in the HadGEM2-ES earth-system model: Radiative impact and climate response, *Atmos. Chem. Phys.*, *12*, 10,887–10,898, doi:10.5194/acp-12-10887-2012.

Jones, A., J. Haywood, and O. Boucher (2009), Climate impacts of geoengineering marine stratocumulus clouds, *J. Geophys. Res.*, *114*, D10106, doi:10.1029/2008JD011450.

Jones, A., J. Haywood, and O. Boucher (2010), A comparison of the climate impacts of geoengineering by stratospheric SO_2 injection and by brightening of marine stratocumulus cloud, *Atm. Sci. Lett.*, *12*(2), 176–183, doi:10.1002/asl.291.

Jones, A., et al. (2013), The impact of abrupt suspension of solar radiation management (termination effect) in experiment G2 of the Geoengineering Model Intercomparison Project (GeoMIP), *J. Geophys. Res. Atmos.*, *118*, 1–10, doi:10.1002/jgrd.50762.

Korhonen, H., K. S. Carslaw, and S. Romakkaniemi (2010), Enhancement of marine cloud albedo via controlled sea spray injections: A global model study of the influence of emission rates, microphysics and transport, *Atmos. Chem. Phys.*, *10*, 4133–4143, doi:10.5194/acp-10-4133-2010.

Kravitz, B., A. Robock, O. Boucher, H. Schmidt, K. E. Taylor, G. Stenchikov, and M. Schulz (2011), The Geoengineering Model Intercomparison Project (GeoMIP), *Atm. Sci. Lett.*, *12*, 162–167, doi:10.1002/asl.316.

Kravitz, B., et al. (2013), Climate model response from the Geoengineering Model Intercomparison Project (GeoMIP), *J. Geophys. Res. Atmos.*, *118*, 8320–8332, doi:10.1002/jgrd.50646.

Latham, J. (1990), Control of global warming?, *Nature*, *347*, 339–340.

Latham, J. (2002), Amelioration of global warming by controlled enhancement of the albedo and longevity of low-level maritime clouds, *Atm. Sci. Lett.*, *3*(2-4), 52–58, doi:10.1006/asle.2002.0099.

Latham, J., et al. (2008), Global temperature stabilization via controlled albedo enhancement of low-level maritime clouds, *Phil. Trans. Roy. Soc. A*, *366*(1882), 3969–3987, doi:10.1098/rsta.2008.0137.

Latham, J., et al. (2012), Marine cloud brightening, *Phil. Trans. Roy. Soc. A*, *370*, 4217–4262, doi:10.1098/rsta.2012.0086.

Lenton, T. M., and N. E. Vaughan (2009), The radiative forcing potential of different climate geoengineering options, *Atmos. Chem. Phys.*, *9*, 5539–5561.

Lewis, E. R., and S. E. Schwartz (2004), *Sea Salt Aerosol Production: Mechanisms, Methods, Measurements and Models – A Critical Review*, Geophysical Monograph Series, vol. 152, 413pp. American Geophysical Union, Washington D.C., doi:10.1029/GM152.

Parkes, B., A. Gadian, and J. Latham (2012), The effects of marine cloud brightening on seasonal polar temperatures and the meridional heat flux, *ISRN Geophysics*, *2012*, 142872, doi:10.5402/2012/142872.

Partanen, A.-I., et al. (2012), Direct and indirect effects of sea spray geoengineering and the role of injected particle size, *J. Geophys. Res.*, *117*, D02203, doi:10.1029/2011JD016428.

Pringle, K. J., et al. (2012), A multi-model assessment of the impact of sea spray geoengineering on cloud droplet number, *Atmos. Chem. Phys.*, *12*, 11,647–11,663, doi:10.5194/acp-12-11647-2012.

Rap, A., et al. (2013), Natural aerosol direct and indirect radiative effects, *Geophys. Res. Lett.*, *40*, 3297–3301, doi:10.1002/grl.50441.

Rasch, P. J., J. Latham, and C.-C. Chen (2009), Geoengineering by cloud seeding: Influence on sea ice and climate system, *Environ. Res. Lett.*, *4*, 045112, doi:10.1088/1748-9326/4/4/045112.

Rosenfeld, D., R. Lahav, A. Khain, and M. Pinsky (2002), The role of sea spray in cleansing air pollution over ocean via cloud processes, *Science*, *297*, 1667–1670, doi:10.1126/science.1073869.

Rosenfeld, D., et al. (2008), Flood or drought: How do aerosols affect precipitation?, *Science*, *321*, 1309–1313, doi:10.1126/science.1160606.

Rudich, Y., O. Khersonsky, and D. Rosenfeld (2002), Treating clouds with a grain of salt, *Geophys. Res. Lett.*, *29*(22), 2060, doi:10.1029/2002GL016055.

Salter, S., G. Sortino, and J. Latham (2008), Sea-going hardware for the cloud albedo method of reversing global warming, *Phil. Trans. R. Soc. A*, *366*, 3989–4006, doi:10.1098/rsta.2008.0136.

Schmidt, G. A., et al. (2006), Present day atmospheric simulations using GISS ModelE: Comparison to in situ, satellite and reanalysis data, *J. Clim.*, *19*, 153–192, doi:10.1175/JCLI3612.1.

Taylor, K. E., R. J. Stouffer, and G. A. Meehl (2012), An overview of CMIP5 and the experiment design, *Bull. Amer. Meteor. Soc.*, *93*, 485–498, doi:10.1175/BAMS-D-11-00094.1.

Tilmes, S., et al. (2013), The hydrological impact of geoengineering in the Geoengineering Model Intercomparison Project (GeoMIP), *J. Geophys. Res. Atmos.*, doi:10.1002/jgrd.50868.

Twomey, S. (1974), Pollution and the planetary albedo, *Atmos. Environ.*, *8*, 1251–1256.

Twomey, S. (1977), The influence of pollution on the shortwave albedo of clouds, *J. Atmos. Sci.*, *34*, 1149–1152, doi:10.1175/1520-0469(1977)034<1149;TIOPOT>2.0.CO;2.

Wang, H., and G. Feingold (2009a), Modeling open cellular structures and drizzle in marine stratocumulus. Part I: Impact of drizzle on the formation and evolution of open cells, *J. Atmos. Sci.*, *66*, 3237–3256.

Wang, H., and G. Feingold (2009b), Modeling open cellular structures and drizzle in marine stratocumulus. Part II: The microphysics and dynamics of the boundary region between open and closed cells, *J. Atmos. Sci.*, *66*, 3257–3275.

Wang, H., P. J. Rasch, and G. Feingold (2011), Manipulating marine stratocumulus cloud amount and albedo: A process-modelling study of aerosol–cloud-precipitation interactions in response to injection of cloud condensation nuclei, *Atmos. Chem. Phys.*, *11*, 4237–4249, doi:10.5194/acp-11-4237-2011.

Watanabe, S., et al. (2011), MIROC-ESM 2010: Model description and basic results of CMIP5-20c3m experiments, *Geosci. Model Dev.*, *4*, 845–872, doi:10.5194/gmd-4-845-2011.

Wigley, T. M. L. (2006), A combined mitigation/geoengineering approach to climate stabilization, *Science*, *314*(5798), 452–454, doi:10.1126/science.1131728.

Wunsch, C. (2005), The total meridional heat flux and its oceanic and atmospheric partition, *J. Clim.*, *18*, 4374–4380.